INFORMATION SCIENCE

SIGNAL PROCESSING AND ERROR REDUCTION FOR RECIPROCATING TRIBOELECTROMETRY

Horia-Nicolai TEODORESCU[1,2], Yopa PRAWATYA[3], Thami. ZEGHLOUL[3], Lucian DASCALESCU[3]

[1]Romanian Academy – Iasi Branch, Bd Carol I nr. 8
[2] "G. Asachi" Technical University, 67, Bd. D. Mangeron, 70050 Iasi, Romania
[3]PPRIME Institute, CNRS – University of Poitiers – ENSMA, 4 av. Varsovie, 16021 Angoulême, France
Corresponding author: Horia-Nicolai TEODORESCU, e-mail: `hteodor@etti.tuiasi.ro`

Abstract. The measurement of the friction coefficient is essential to numerous applications, including mechanisms and tribocharging assessments. There are several families of measuring devices using various measuring principles, configurations and types of movements. We analyze in detail the potential measurement error sources in the devices falling in one of these classes and exemplify these errors for the case of a custom-made device. The use of the method of the horizontally sliding cartridge (also named in the article sledge or shuttle) with vertical force applied to the probe, and of other similar setups for friction force and friction coefficient measurement raises several obstacles. Among these are the compensation of the effect of the involved masses and of the frictions between the cartridge and the measuring table, of the mass and frictions in the displacement sensor, moreover the estimation of the mechanical noise in the sliding process. We analyze the involved factors, exemplify the analysis with measured signals, propose a compensation method, and apply it to a measuring setup in order to reduce measurement errors. The analysis and the related method for error compensation are appropriate for and easily adaptable to a large class of measurement setups.

Key words: signal processing, measurement errors, triboelectrometer, error compensation, dynamics, sliding contact, friction.

1. INTRODUCTION

Triboelectrometry is defined here as the assessment of the tribelectric effect. The measurement of the friction is a necessary step in triboelectrometry. There are numerous methods for measuring the friction forces, using various experimental setups, including the common inclined plane method and the horizontal plane method [1, 2]. Several of these methods are described in detail only in patents, such as [3–5]. In all these methods and devices, there are several error factors affecting the derivation of the true friction force between the samples under investigation. While the literature discusses a number of error sources, for example vibrations induced by friction [6–8], sensor misalignment and contact nonuniformity [9] it is unclear how these errors affect the measurements using the various commercial tribometers, and how the errors, if any, are compensated in commercial devices; we were unable to find such information in the documentations available for some of these tribometers. However, it is known that precise measurement of the kinetic friction requires the use of vibration isolation techniques and the use of several sensors to measure and then compensate for accelerations induced by undesired movements (vibrations induced by movement with friction) [6].

There is no commercial equipment today for triboelectrometry. The setup we used was conceived with the aim to measure triboelectric charging for pairs of polymeric samples (slabs) [10–12]. The setup belongs to the reciprocating class of tribometric devices and was not designed for determining the friction coefficient between the samples. Therefore, the friction forces can be determined only indirectly and with certain approximations.

For assessing the triboelectric effect it is desirable to determine the workforce performed by the friction force between the samples under friction. However, other friction forces occur in the setup, while the forces directly measurable are not equal to the friction force of interest, but to a sum of inertial and friction forces.

This requires kinematic analysis and the identification of the independent variables. However, various causes, including imperfections of mechanisms and variability of the friction between the samples under analysis introduce errors that must be minimized.

While we detail and exemplify the computation and compensation methods for a specific case, they remain largely valid for a whole class of measuring setups that are suitable for characterizing the triboelectric effect. Indeed, all such setups involve the measurement of the tangential and normal forces during friction, and the two samples under friction need some kind of holders, at least one of them moving together with one of the samples. Such setups for the measurement of the triboelectric effect involve forces as in our model, whatever different movement is used in those setups. Therefore, the analysis and model in this study can easily be generalized to cases from similar methods of measuring the triboelectric effect. In addition, various methods for measuring friction forces involve similar forces, including inertial forces; an example is that of measuring friction between pistons and rings, [13], where the calculation of inertial forces is an intermediate step for deriving the friction forces and strain gages are used to measure transmitted forces. We also analyze the sources of errors and expose a method for minimizing the errors.

2. DESCRIPTION OF THE MEASURING SETUP

The basic experimental setup for triboelectric charging measurements was described in detail in [10] and [11]; the main difference in the setup described in this paper is that the movement is produced by a linear motor and the movement is essentially at constant velocity. The experimental set up consists in the electromechanical bench for sample tests, the electric potential measurement apparatus, and the annex devices for temperature mapping [11]. Details on the measuring method and several issues related to data processing were presented in [10] and [14] and are not repeated here.

The mechanical part of the setup includes a horizontally sliding sample holder that supports one of the samples measured; the other sample is maintained fixed by a second sample holder and pressed upon the former sample (Fig. 1). The normal force of direct interest is exerted on the fixed sample during the movement of the mobile sample carried by the cartridge. A controlled linear motor moves the cartridge; a force sensor determines the tangential (motor) force, while another force sensor determines the normal force F_{ns} and its (undesired) variation. A displacement sensor connected to the cartridge determines the displacement of the moving sample.
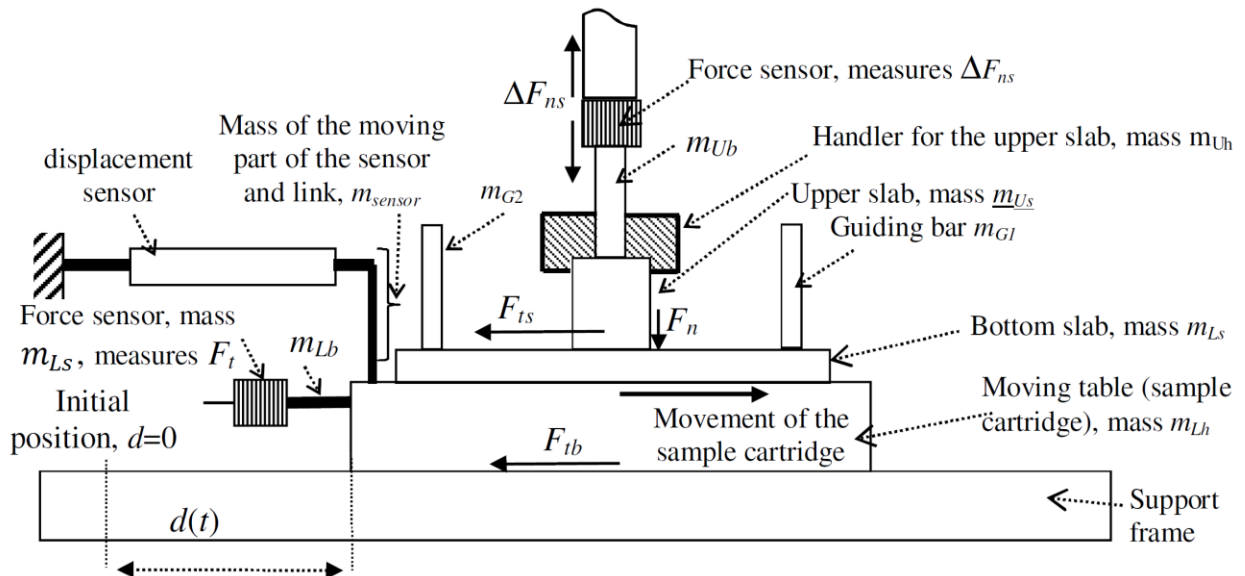

Fig. 1 – Sketch of the setup with the acting forces and displacement direction. Notations in the text.

Friction occurs between several of the elements in the setup. A major tangential force F_t component is the friction F_{cF} between the cartridge and the frame of the setup. Also, the displacement sensor, when it is mechanical, contributes a friction force, F_{fs}. The friction [6] and small deficiencies in the moving mechanism introduce fluctuations of the tangential force, n_{Ff}. Imperfect planarity and friction introduce variations in the normal force. One normal and one tangential force are measured with two sensors placed as in Fig. 1. The masses in Figure 1 are given in Annex 1.

3. ANALYSIS OF THE DYNAMICS OF THE TRIBOMETRIC SYSTEM

3.1. TANGENTIAL FORCES

During the displacement of the mobile slab and cartridge all measured quantities are time varying. The measured quantities include the tangential force $F_t(t)$ applied to the moving cartridge with the sample, see Fig. 1, the normal force $F_n(t)$ applied to the samples, the time variable displacement $d(t)$ of the moving table, the electrical potential and the temperature map of the bottom sample immediately after the friction. The total tangential force measured includes the sum of the two friction forces, the friction force between the measured slabs, F_{ts}, and the friction force between the measuring table and the measuring bank, F_{tb}, shown in Fig. 1, and of the tangential inertial force, $F_{t\text{-}inertial}(t)$, associated with the moving parts, namely the lower slab, the lower slab cartridge, and the moving part of the sensor,

$$F_t(t) = Fts(t) + F_{tb}(t) + F_{t\text{-}inertial}(t). \tag{1}$$

The friction force $F_{ts}(t)$ corresponds to the friction of interest, between the two samples, while $F_{tb}(t)$ stands for the friction between the moving (lower) cartridge and the supporting frame of the setup plus the friction in the displacement sensor, between its fixed and moving part (the later one being neglected subsequently). The values of F_{tb} are estimated by "blank" tests, that is with no normal force applied to the shuttle. The inertial force corresponds to the masses $m_{Lh} + m_{Ls} + m_{Lb} + m_{sens}$, where m_{Lh} is the mass of the lower sample holder (shuttle), m_{sens} is the mass of the moving part of the displacement sensor and of the link from that part of this sensor to the moving cartridge, m_{Ls} is the mass of the tangential force sensor, and m_{Lb} is the mass of the bar connecting the tangential force sensor.

3.2. NORMAL FORCE

The normal force F_n of primary interest is the force applied between the samples, not the measured normal force $\Delta F_{ns}(t)$. In the setup, the sensor is pulled in both directions by two vertical forces, one tending to lift the upper sample holder and the other the sum of the weights of the upper holder, gm_{Uh}, of the upper bar, gm_{Ub}, of the upper sample, gm_{Us}, and of the two guiding bars, $g(m_{G1}+m_{G2})$. We neglect frictions of the guiding bars in their guides. Therefore, the total normal force is

$$Fn(t) = -\Delta Fns(t) + g(m_{Uh} + m_{Us} + m_{G1} + m_{G2}). \tag{2}$$

The normal force is measured with a sensor placed as in Fig. 1 and, excluding vibrations, this force includes no inertial component. During all tests, the nominal value of the masses in (2) was computed as $m_1 + m_2 + m_3 + m_4 + m_{Us} = 1.551 \pm 0.01 kg$, where the variation of 0.01 kg is due to the variable mass of the samples used. The "virtual instrument" was zeroed for $g(m_{Uh} + m_{Us} + m_{G1} + m_{G2})$. The nominal value of ΔF_{ns} was 10 N. Therefore, the nominal value of the normal force contributing to friction was 4.71 N (approximated in computations by 5 N).

Using these details on the normal force, the tangential force can be detailed as follows. The measured tangential force, beyond the sum of forces in (1), includes a noise component, η_t and a systematic error (offset), η_{toff}, due to the sensor zeroing. For reciprocating tribometers, the offset is easy and precisely removed by computation of the average over several cycles. The full expression of the tangential force is

$$F_t(t) = F_{ts}(t) + F_{tb}(t) + M_t \cdot a_h(t) + a_h(t) + \eta_t(t) + \eta_{toff}, \tag{3}$$

where M_t is the mass of all elements moving horizontally and $a_h(t)$ is their acceleration in the horizontal direction, assuming equal accelerations for all these elements. The forces F_{ts} and F_{tb} are produced between different surfaces, see Fig. 1, and have the expressions

$$F_{ts}(t) = F_n(t) \cdot \mu$$
$$F_{tb}(t) = (F_n(t) + M_t(g + a_v(t) + \eta_n)) \cdot \mu_0 \tag{4}$$

$$F_{tb}(t) = (F_n(t) + M_t(g + a_v(t) + \eta_n)) \cdot \mu_0, \tag{5}$$

where μ is the coefficient of friction (COF) specific to the couple of slabs, assumed constant at constant velocity, F_n is the normal force (2) applied to the slabs, μ_0 is the COF specific to the contact surfaces of the moving table and the frame of the measuring bank, and $a_v(t)$ is the vertical acceleration of the mass M_t during the movement of the lower cartridge (unloaded); g is the gravitational acceleration and η_n is an acceleration noise along the normal direction. The acceleration $a_v(t)$ differ for the case when the lower cartridge is unloaded (*i.e.*, not pressed by a normal force) and for the case the lower cartridge is loaded; we denote these accelerations respectively by $a_{v0}(t)$ and $a_{v1}(t)$. During blank tests, when the setup is not loaded with a normal force, the component $F_{tb}(t)$, denoted by $F_{tb0}(t)$, is

$$F_{tb0}(t) = M_t(g + a_{v0}(t) + \eta_{n0})\mu_0, \tag{6}$$

where η_{n0} is the acceleration noise with the cartridge unloaded.

Examples of variations of the measured tangential force $F_t(t)$, of the measured normal force $\Delta F_{ns}(t)$, and of the measured displacement $d(t)$ are shown in Fig. 3. The waveforms for all three signals representing forces are quasi-periodical, with similar but non-repeatable forms. The graphs include raw data, with uncorrected offsets; the reciprocating movement allows us to better correct the offsets and drift by computations (in software) than by trimming as detailed in the next sections.

(a) displacement $d(t)$

(b) normal force $\Delta F_{ns}(t)$ examples
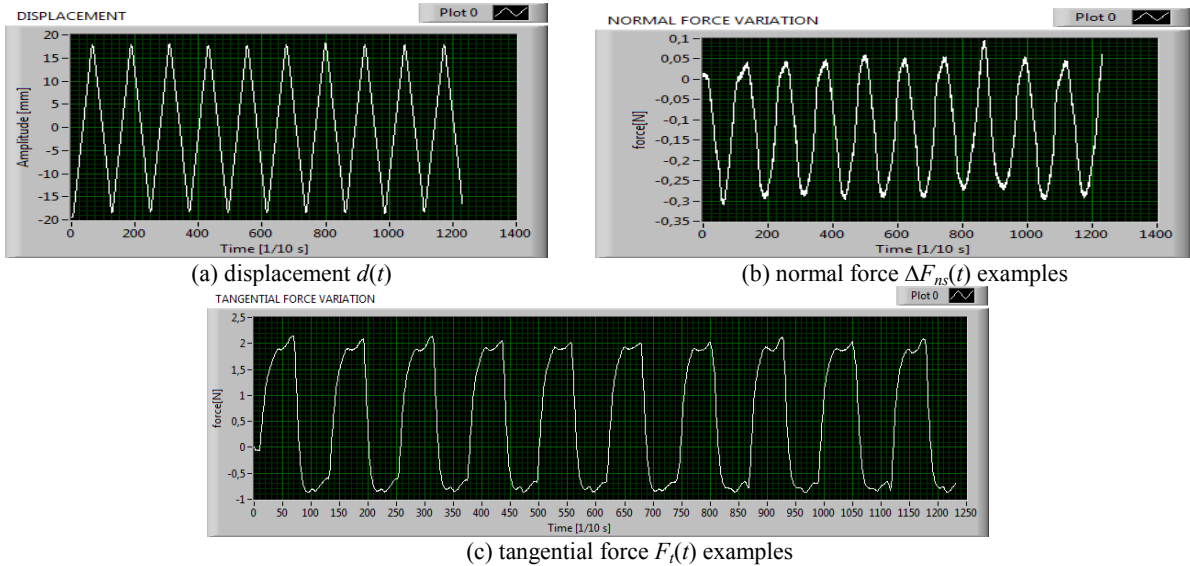
(c) tangential force $F_t(t)$ examples

Fig. 2 – Examples of time-dependent variation of the measured quantities, the tangential and normal forces and the corresponding displacements, for normal (loaded) tests.

While the normal force is supposed to be constant, the small variations of the thickness of the lower sample (as reported in [10]) and the vibrations due to movement with friction [6] produce a significant variation of the normal force, of about 0.5 N peak-to-peak (Fig. 3). For reasons explained in the next Section, measurements of the quantities $F_t(t)$, $\Delta F_{ns}(t)$, and $d(t)$ were also performed with the lower sample removed, that is, without a normal force applied to the lower holder. This type of test is named blank test throughout the paper.

4. SIGNAL PROCESSING AND DATA ANALYSIS

4.1. ANALYSIS OF SLAB ROUGHNESS AND NOISE COMPENSATION

The samples consisted of slabs of polymeric, industrial grade materials (industrially manufactured). The slabs were cut from large sheets of PVC, ABS, and polystyrene (PS), taking precautions not to produce before testing any scratches on the surfaces to be tested. The materials under friction have been in the experiments: (1) PVC for the lower sample and ABS for the upper sample; (2) PVC for the lower sample against PS; (3) PVC against PVC.

Before tribocharging, the samples have been assessed for roughness. The roughness profile is important because it induces noise in the tangential force and possibly minute vertical movements of the upper (pressing) slab and thus further small, noise-like variations of the friction force. An example of roughness profile for a PVC slab used in experiments is shown in Fig. 2.
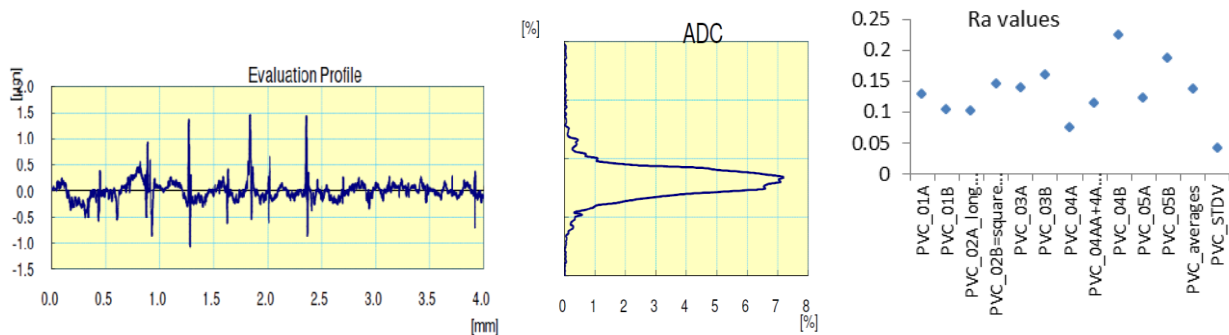
Fig. 3 – Example of roughness profile and ADC profile of roughness, slab of PVC. (Standard ISO 1997, Profile R, λ_s = 2.5 μm, cut-off at 0.8 mm, Gauss filter, R_a = 0.129 μm, R_q = 0.184 μm, R_z = 1.496 μm.) (DigitalSurf™ measuring device.) PVC_*** are samples of PVC slabs of various shapes and sizes, employed in the experiments.

For all experiments reported in this study, the movement conditions (nominal) were: displacement along 50 mm (comparable to other tribometers in the literature); displacement speed 15 mm/s; we recall that the normal force on the sample (under static conditions) was about 5N. The error sources discussed throughout the paper affect the nominal conditions; some of these errors are common to many tribometers [6].

The problem is to obtain an estimation of the average of μ for a given sample from the above expression and from the statistics of the measured data. Notice that we need an average per sample and are not interested here in the local variation of the coefficient of friction. We assume that all the masses are known precisely. When the mass of the lower sample, m_{Ls}, is significant with respect with the mass of the cartridge m_{Lh}, one needs to replace m_{Lh} with $m_{Lh} + m_{Ls}$ for the situation (not the "blank") of measurement. In this case, we assume that m is also precisely known. The tangential force and displacement during blank cycles are exemplified in Figs. 4a,c and Fig. 5a.

Examples of recorded data and of the derivation of the velocity and acceleration are shown in Figs. 5a,b. In all figures representing recorded data, the time (on the horizontal axis) is replaced with the number of the signal sample, with counting starting at 1; the sampling period (time between two samples) is 0.1 s in all figures.

While the Fig. 4c seems to indicate an instantaneous change of velocity, which is a physical impossibility, an enlarged space-time plot (Fig. 5a) and the plot of velocity and acceleration (Fig. 5b) indicate a slow change in velocity and a noisy displacement. Also, a plot of the normal force shows a significant level of noise (Fig. 6), which partly explains the noise in the acceleration through variation of the friction force. This noise contributes an instantaneous error in the normal force up to 0.39N/5N≈8%. Part of the noise is due to the roughness illustrated in Fig. 2.
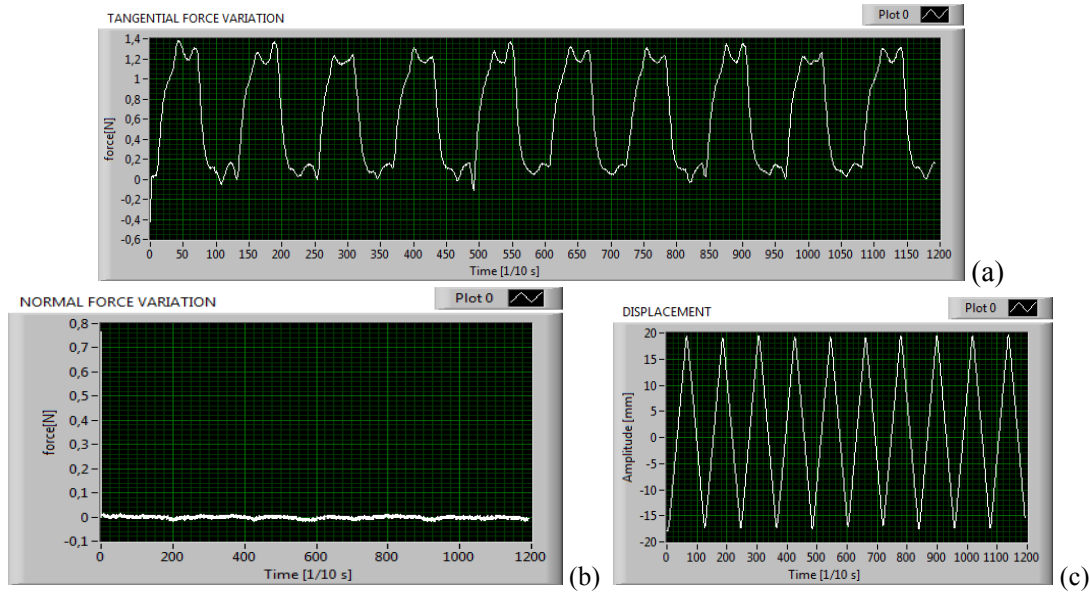
Fig. 4 – Unloaded (blank test): a) measured tangential force; b) measured normal force; c) displacement, period 3.3 s.
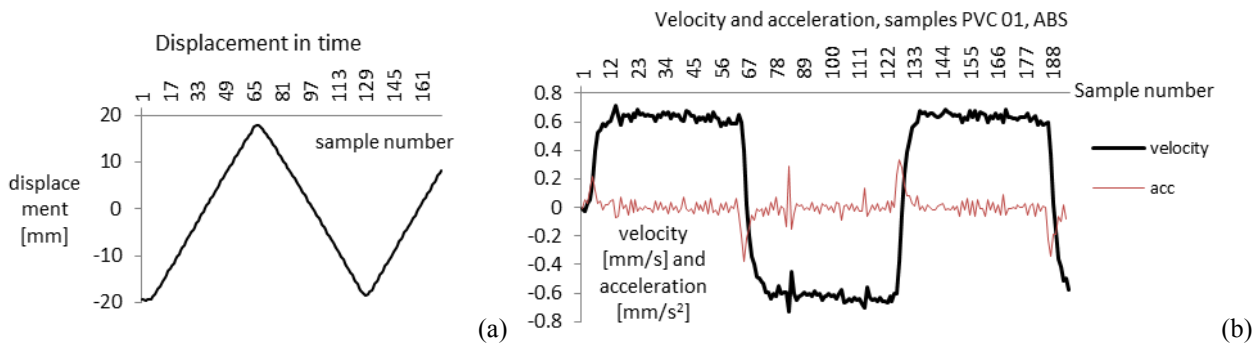

Fig. 5 – a) Rounded turns in the displacement graph, allowing for finite accelerations (finite inertial forces); b) example of velocity and acceleration graphs, computed. Sample of PVC (square) sliding vs. slab of ABS along the surface striations.
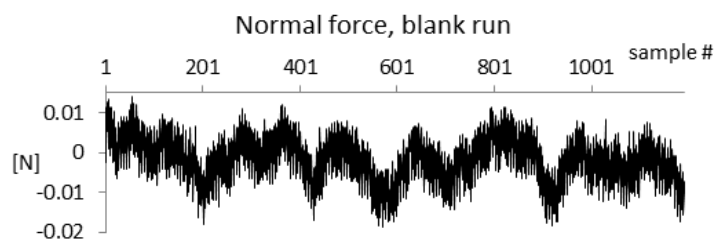

Fig. 6 – Noisy normal force measurement during blank tests.

The presence of the noise in the tangential force $F_t(t)$ is proved by "blank" tests, where the measured slab is removed, therefore the moving cartridge is unloaded, $F_n(t) = 0$. The small variable signal $F_n(t)$ detected during blank tests (Figs. 4b and 6) has the characteristics of a typical noise. The measured signal $F_t(t)$ is non-repetitive from cycle to cycle; the variable component of $F_t(t)$ with respect to the "average cycle" defined subsequently is considered noise. Because in case of the considered measuring setup the movement is alternative and the tangential force proves to be not symmetrical with respect with the moment of movement reversal, we consider complete reciprocating movement cycles (alternate, forth and back movements).

4.2. COMPENSATION FOR THE AVERAGE ERRORS
IN DETERMINING THE TANGENTIAL FORCE DUE TO LOADING

Next, a method to determine the average cycle during blank tests is exposed with the aim of determining the component F_{tb}. We determined the cycles between successive zero crossing moments where the tangential force reverse sign passing from positive to negative values; this is done with the composed condition $F_n(T_{k-1}) > 0$, $F_n(T_{k-1}) < 0$, and the value $F_t(T_{k-1}) \approx 0$ is selected. The values $T_{k+1} - T_k$ represent the duration of the kth (pseudo-)period of F_n. Then, we averaged the cycles taking for every moment t_n, $0 \leq t_n \leq \max_k (T_k)$ the average of $F_t(n+T_k)$ for all k values, including for the first period $F_t(n)$. In this way, we obtained the average $<F_t(n)>$ which we deduced from the signal corresponding to periods in the $F_t(t)$ signal measured with friction (loaded sample). However, the two signals (for the unloaded and loaded conditions) are not time-aligned. Therefore, the subtraction was performed after alignment, defined by the maximum of the cross-correlation function of the two signals.

The compensation method described above can be seen as a local compensation method, as it applied to each original sample a specific compensation based on a reconstructed cycle during blank tests, the average blank cycle being subtracted, sample by sample, from the measured data. The tangent force averaged over 5 periods, according to this method, is shown in Fig. 7. It corresponds to the phase plot in Fig. 8.
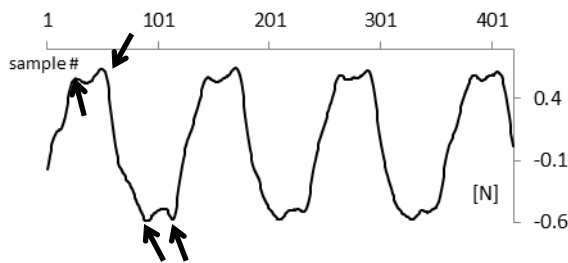

Fig. 7 – Tangent force signal (unloaded measuring system) averaged over 5 periods, with average of the signal nulled.
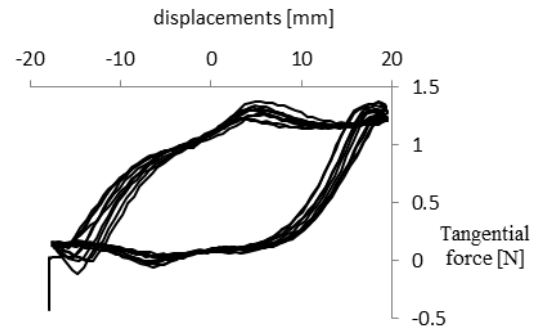
Fig. 8 – Phase plot for the dynamics of the unloaded measuring system (offset not removed).

The averaging shows that there are significant differences even between moving averaged periods. The peaks indicated by arrows in Fig. 7 show an increase of the tangential force at the end of the movement, when acceleration is high. The phase plot for the initial (measured) F_t *vs.* displacement, for the case of unloaded setup, is shown in Fig. 8. Also, the graph, which is a typical phase diagram as used in system dynamics studies, shows that the process is actually a chaotic one.

A simpler method of determining the approximate tangential force is to select on the phase diagram the regions of almost horizontal traces and to average over them, then subtract the resulted values from the data. The conditions for selecting the regions of almost constant force for the loaded system have been set manually at $F(t) > 1.5$ N and $F(t) < -1.5$ N.

The conditions for selecting the regions of almost constant force for the blank (unloaded) system have been $F(t) < -0.4$ N simultaneously with $-10 < d < -5$ and respectively $F(t) > 0.4$ N simultaneously with $3 < d \geq 12$. Notice that the upper and lower branches in the phase diagram, corresponding to the two directions of movement, are significantly different; the lower branch has a larger displacement distance where the force is almost constant.

Figures 8 and 9 show that, for both the unloaded and the loaded cycles, the force F_t is less variable toward the end of a semi-cycle and varies strongly during the first half of the semi-cycles. Therefore, the last half of the semi-cycles is considered for obtaining the average of the tangential force at constant acceleration (the part that is due to the friction F_{tb} and subsequently to derive the value of μ.

However, the upper branch of the cycle and the lower branch of the cycle of the unloaded system differ considerably. Hence, the error they introduce when used as a basis to compensate the movement with friction is much larger for the upper branch. We use only the lower branch of the cycles for compensation.
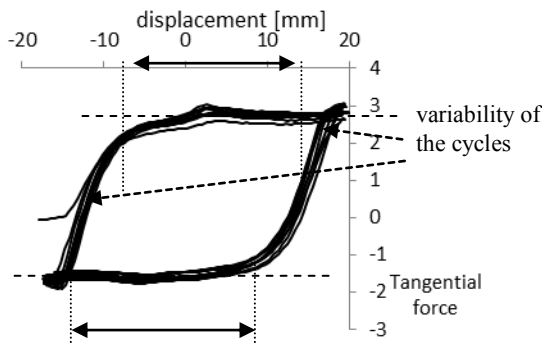
Fig. 9 – Phase plot for the dynamics of the loaded (normal force present) measuring system. Measurement with reference not set to zero (offset).

The intervals marked by double arrows in Fig. 9 show the space intervals where the tangential force is almost constant and therefore the intervals where the average friction force is preferably computed. These average values of the forces are then subtracted from the data.

Notice that the phase diagram for PVC parallel *vs.* ABS shows also a chaotic, yet more regular behavior, as illustrated in Fig. 9.

This method of compensation is global, in the sense that it determines an average force per semi-cycle from the blank test and subtracts it from the data.

5. RESULTS AND DISCUSSION

The determination of the tangential force during blank tests allows us to compensate for it. However, the compensation without proper alignment between the time series produces rough results (Fig. 10). After proper alignment, the compensated time series for the tangential force clearly indicates that the maximal force occurs at the ends on the reciprocated movement, where the accelerations are higher, as expected. The regions between the positive and negative peaks would ideally be plateaus; the variations of the force during these intervals indicate variability of the friction and noisy changes in the normal force. Notice that, compared to the original traces (Fig. 11), which wrongly indicate a maximal tangential force during the intervals of constant velocity movement; the compensated cycles indicate correctly the peaks of the tangential force (Fig. 10). Figure 11 clearly demonstrate the need for a correct alignment between the force and displacement time series, because a shift between them is possible because of mechanical imperfections in the mechanism of the measuring setup.
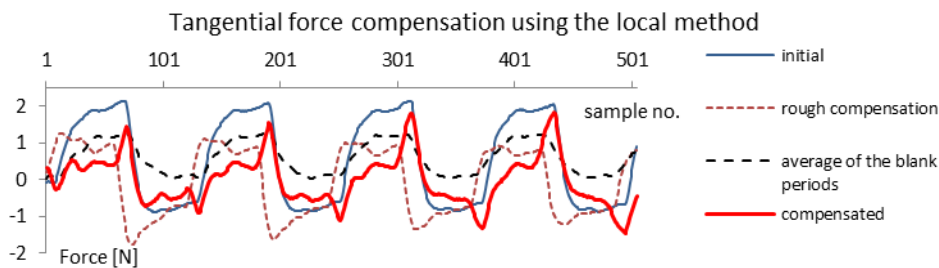

Fig. 10 – Compensation of the tangential force signal using the averaged cycles (moving average over 5 cycles).
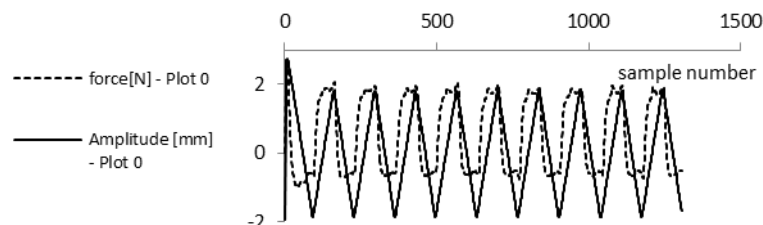

Fig. 11 – Example of phase difference between the measured tangential force (dotted line) and the displacement (solid line, scale 1:10). Data correspond to friction between a PVC sample *vs.* ABS sample.

There are several difficulties in automatically applying the first compensation method. Figures 7, 8, and 9 show that the loops have not the same "end" (upper and lower returning point, see arrow). Also, if one

makes a vertical section of the loops, the same branch of the loop does not intersect the branches at the same point on all cycles (as happens for any pseudo-periodic or chaotic system). Therefore, "periods" are unequal. Thus, one period of the unloaded system cannot be used as perfect compensation for all "periods" of the loaded system. We need to use several average templates, with different quasi-periods, of the unloaded system and try to match with them a specific "period" of the loaded system.

Notice that the cycles of the unloaded system are significantly less smooth than the cycle of the loaded system, because no normal force keeps the moving table in good contact with the frame of the setup, allowing vertical movement of the bank and thus a variable friction force.

In case of the second method, the number of samples used to compute the average of the negative component of the tangential force has been 230, with an average of –0.558; 140 samples were found satisfying the conditions for the positive branch, while the positive branch average was found 0.612. While the numbers of samples obtained for compensation on the two semi-cycles differ, they are easily counted; thus, the second method is easy to automate.

6. CONCLUSIONS

The study revealed that inherent mechanical imperfections of the friction and triboelectric measuring devices may be partly compensated by performing blank tests and using the results of these tests to compute the error compensations. The blank tests show that the friction of the sledge in the frame may have an important role and must be taken into account in the computation of the tangential force and hence in the determination of the friction force. The reciprocating operation brings errors at the ends of the strikes. These errors can be removed by taking into account only the movement during the time intervals when the displacement is performed without horizontal accelerations. The determination of the friction coefficient, required in triboelectric experiments for correlating the influence of this variable on the dependent variable of the charging raises several computational and experimental difficulties that currently limit the determination only along parts of the reciprocating movement, where velocity and tangential forces are almost constant.

The two methods of estimation of the tangential force and of the friction coefficient, one based on compensation with the averaged cycles during unloaded pre-tests and the other based on the smooth horizontal intervals in the phase diagrams, have both drawbacks related to the errors they incur. However, their use much improves the correctness of the estimations of the friction force. Thus, the correction methods presented must be included in the software for tribometers and triboelectric characterization devices. The errors in the sample surface alignment, mentioned previously in the literature and found also in this study can be reduced by statistical averaging.

Further work is needed to reduce the looseness in the joints from the motor to the shuttle, while keeping accelerations and forces at reasonable levels; this would reduce the length of the displacement that is affected by high uncertainties. Also, the measuring setup should be equipped with accelerometers both for monitoring the measuring conditions and for compensating vibrations. The conjoint use of accelerometers and piezoelectric actuators for active damping of the vibrations along both axes would further improve the precision of the measurements.

Authors' contribution. Yopa PRAWATYA and Horia-Nicolai TEODORESCU performed the experiments. Horia-Nicolai TEODORESCU proposed the study and processed most of the data. Several drafts of the paper were written by Horia-Nicolai TEODORESCU. All authors discussed and interpreted the results and contributed to writing the final version of the paper.

Annex 1

The masses of the parts in Fig. 1 are (in grams) $m_{Lh} = 3\ 701$; $m_{Ls} \approx 40–50$; $m_{Uh} = 942$; $m_{Us} \approx 40–50$; $m_{G1} = 284$; $m_{G2} = 263$; $m_{Ub} = 12$.

REFERENCES

1. N. AXÉN, S. HOGMARK, S. JACOBSON, *Friction and wear measurement techniques* (Ch. 13), in: B. Bhushan (Ed.), *Modern Tribology Handbook*, Vol. 2, CRC Press, Dec 28, 2001.
2. S. HOGMARK, S. JACOBSON, M. LARSSON, U. WIKLUND, *Mechanical and tribological requirements and evaluation of coating composites* (Ch. 26), in: B. Bhushan (Ed.), *Modern Tribology Handbook*, Vol. 2, CRC Press, 2001.
3. United States Patent Application 20120010827, *Friction test apparatus and methods for antiperspirant/deodorant products*, Yarlagadda; in: T.T. (Inventor), Jan. 12, 2012.
4. United States Patent 7,614,275, *Method and apparatus for determining coefficient of friction*, Lin *et al.*, Nov 10, 2009.
5. B.A. KRICK, W.G. SAWYER, *A little analysis of errors in friction for small wear tracks*, Tribol. Lett. **39**, pp. 221–222, 2010.
6. P. L. KO, C. A. BROCKLEY, *The measurement of friction and friction-induced vibration*, J. of Lubrication Technology, **92**, *4*, pp. 543–549, 1970.
7. N. KADO, C. TADOKORO, K. NAKANO, *Kinetic friction coefficient measured in tribotesting: Influence of frictional vibration*, Tribology Online, **9**, *2*, pp. 63–70, 2014, DOI 10.2474/trol.9.63, 2014 Japanese Society of Tribologists.
8. A.G. PLINT, *Friction force measurement in reciprocating tribometers*. STLE 2011, http://www.phoenix-tribology.com/wp-content/uploads/guidance/Guidance-Dynamic-Friction-Force.pdf.
9. M.A. SIDEBOTTOM, B.A. KRICK, *Transducer misalignment and contact pressure distributions as error sources in friction measurement on small-diameter pin-on-disk experiments*, Tribology Letters, **58**, 2, pp. 1–6, 2015.
10. B. NEAGOE, H.-N. TEODORESCU, Y. PRAWATYA, L. DASCALESCU, T. ZEGHLOUL, *Experimental bench for studying the relation between the dynamic characteristics of the frictional motion and the electric potential at the surface of polymer slabs in sliding conformal contact*, Tribology International, **111**, pp. 107–115, 2017.
11. B NEAGOE, Y PRAWATYA, T ZEGHLOUL, D SOUCHET, L DASCALESCU, *Laboratory bench for the characterization of triboelectric properties of polymers*, Journal of Physics: Conference Series, **646**, 1, 012058, 2015.
12. Y. E. PRAWATYA, M. B. NEAGOE, T. ZEGHLOUL, L. DASCALESCU, *Surface-Electric-Potential Characteristics of Tribo- and Corona-Charged Polymers: A Comparative Study*, IEEE Trans. Industry Applications, **53**, *3*, pp. 2423–2431, 2017.
13. URAS, H., PATTERSON, D., *Measurement of piston and ring assembly friction instantaneous IMEP Method*, SAE Technical Paper 830416, 1983; https://doi.org/10.4271/830416.
14. PRAWATYA, SENOUCI *et al.*, *Statistical process control of the tribocharging of polymer slabs in frictional sliding contact*, Proc. Industry Applications Society Annual Meeting (IEEE), 1–5 Oct. 2017, Cincinnati, OH, USA.